Mon. Not. R. Astron. Soc. **327,** 1165–1172 (2001)

Thermal desorption of water ice in the interstellar medium

Helen J. Fraser,[1★†] Mark P. Collings,[1] Martin R. S. McCoustra[1] and David A. Williams[2]
[1]*School of Chemistry, University of Nottingham, University Park, Nottingham NG7 2RD*
[2]*Department of Physics and Astronomy, University College London, Gower Street, London WC1E 6BT*

Accepted 2001 July 5. Received 2001 May 30; in original form 2001 March 21

ABSTRACT

Water (H_2O) ice is an important solid constituent of many astrophysical environments. To comprehend the role of such ices in the chemistry and evolution of dense molecular clouds and comets, it is necessary to understand the freeze-out, potential surface reactivity and desorption mechanisms of such molecular systems. Consequently, there is a real need from within the astronomical modelling community for accurate empirical molecular data pertaining to these processes. Here we give the first results of a laboratory programme to provide such data. Measurements of the thermal desorption of H_2O ice, under interstellar conditions, are presented. For ice deposited under conditions that realistically mimic those in a dense molecular cloud, the thermal desorption of thin films ($\ll$50 molecular layers) is found to occur with zeroth-order kinetics characterized by a surface binding energy, $E_{\rm des}$, of 5773 ± 60 K, and a pre-exponential factor, A, of $10^{30\pm2}$ molecules cm^{-2} s^{-1}. These results imply that, in the dense interstellar medium, thermal desorption of H_2O ice will occur at significantly higher temperatures than has previously been assumed.

Key words: molecular data – molecular processes – methods: laboratory – ISM: molecules.

1 INTRODUCTION

It has become clear over the last decade that purely gas-phase schemes cannot account for the variety and richness of chemistry occurring in the interstellar medium (ISM), particularly in denser regions of molecular clouds where star formation is occurring. In such environments gas–grain interactions must also play a key role (Williams 1998). Within the lifetime of a dense molecular cloud (of the order of 10^6 yr), the grains accrete icy mantles as atomic and molecular species freeze out on to the grains. The ices are processed further by cosmic ray impacts, ultraviolet photolysis and shocks. Consequently, the chemical composition of these icy mantles is significantly different from that of the local gas-phase environment (Rawlings 2000). During cloud collapse and stellar formation the grains are reheated, and molecules are recycled from the solid state into the gas-phase environment. In regions where the H_2O concentrations are depleted, it is assumed that the species is still locked in the icy mantles on the grains, and consequently that the temperature is below the sublimation temperature of the tracer gas (van Dishoeck & van der Tak 2000). When evaluating these environments it is clearly necessary to understand the sublimation behaviour of the ice, and its thermal stability. The surface binding energy, $E_{\rm des}$, and sublimation rates of molecular ices may only be obtained empirically. When combined, these data can be used to determine molecular residence times on the ice surface, in terms of a population half-life as a function of temperature. These data are also applicable in other astronomical environments, such as cometary nuclei and comae, planetary surfaces and satellites.

H_2O is the most abundant molecular ice in dense ISM regions (Ehrenfreund & Schutte 2000). The H_2O ice band at 3.07 μm is detected on lines of sight towards reddened stars that have a visual extinction above a critical value (Whittet 1993), and is typically one of the strongest bands in interstellar infrared spectra. The abundance and morphology of H_2O ice in the ISM are generally inferred from the intensity and line profile of the 3.07-μm band. At low pressures and temperatures, such as those in the ISM, the H_2O ice can exist in both amorphous and crystalline forms. To complicate the picture further, the amorphous ice can exist in both high-density (1.1 g cm^{-3}) and low-density (0.94 g cm^{-3}) forms, reflecting differences in the porosity of the material, with a phase change from former to latter occurring irreversibly between 38 and 80 K (Jenniskens et al. 1995). It is generally assumed that the dominant morphology of icy mantles on interstellar grains resembles that of high-density amorphous ice, with other 'impurity' molecules trapped in the H_2O ice matrix (Jenniskens et al. 1995). This is evident in comparisons of *Infrared Space Observatory* (*ISO*) Short Wavelength Spectrometer (SWS) and ground-based observations with laboratory spectra of mixed ice

★Present address: The Raymond and Beverly Sackler Laboratory for Astrophysics, Sterrewacht Leiden, Leiden University, Postbus 9513, 2300 RA, Leiden, the Netherlands.
†E-mail: fraser@strw.leidenuniv.nl

analogues (Ehrenfreund & Schutte 2000, and references therein). However, laboratory spectra of pure H_2O ices show clear differences in the line profile of the 3.07-μm feature associated with different ice morphologies and temperatures (Jenniskens et al. 1997). It is therefore likely that some H_2O ices have undergone 'mild processing' and recooling (such as gentle heating below 80–100 K, or rapid localized heating because of shocks), and will therefore also exist in low-density amorphous and crystalline forms (Jenniskens & Blake 1994, 1996). The physical properties of the H_2O ice, such as density, conductivity, vapour pressure and sublimation rate, are dictated by its structure. Significant differences are expected between the surface chemistry and bulk behaviour of the ice phases. In addition, the physical and chemical properties of the ice may also be affected by way in which the ice film is deposited, its lifetime, and processing prior to thermal desorption (Sack & Baragiola 1993).

This paper is the first in a series of papers reporting new experimental results on gas–surface interactions occurring under conditions resembling those in the ISM and star-forming regions. With the aid of a purpose-built instrument, we are now able, for the first time, to provide the astrochemical community with experimental results addressing not only desorption energies, but also sticking probabilities and desorption mechanisms. Here we present the results of laboratory studies to determine the surface binding energies on, and sublimation rates of, H_2O ice under interstellar conditions. Previous studies, where the surface binding energies were determined from spectroscopic data, suggested that the surface binding energy of H_2O on H_2O ice was 4815 ± 15 or 5070 ± 50 K, for unannealed and annealed ice samples, respectively (Sandford & Allamandola 1988). It was also presumed that the desorption kinetics of the system were first-order. These data have been used extensively in the astronomical literature, where it is now widely reported that under interstellar conditions H_2O can only exist in the solid phase below about 100 K (Hasegawa & Herbst 1993; Sandford & Allamandola 1993; Ehrenfreund & Schutte 2000). The direct techniques used to determine the surface binding energy in this work are described in Section 2. The results are detailed in Section 3. In these experiments the thermal desorption of thin H_2O ice films is found to occur with zeroth-order kinetics characterized by a surface binding energy, $E_{\rm des}$, of 5773 ± 60 K, and a pre-exponential factor, A, of $10^{30 \pm 2}$ molecules $\rm cm^{-2}\,s^{-1}$. In Section 4, a comparison is made with previous results, from both thermodynamic and spectroscopic techniques, and the astrophysical implications of this work are discussed, focusing on applications associated with dense molecular clouds. The conclusions are summarized in Section 5.

2 EXPERIMENTAL METHOD

The Nottingham Surface Astrophysics Experiment (NoSAE) was designed to measure surface binding energies and sticking probabilities empirically and accurately, recreating the harsh interstellar environment under controlled laboratory conditions. A much fuller description than can be given here is to be found elsewhere (Fraser, Collings & McCoustra 2001). Basically, the experiment consists of a stainless steel ultra-high-vacuum (UHV) chamber with an operating base pressure of 6×10^{-11} torr. The primary constituent (>90 per cent) of this vacuum is H_2, providing very similar conditions with the experiment chamber to those found in the ISM. The chamber is equipped with an effusive gas deposition system, a quadrupole mass spectrometer (QMS), a Fourier Transform Infrared (FTIR) spectrometer and a quartz crystal microbalance (QCM). The QMS is used for temperature-programmed desorption experiments (see Section 2.2), the FTIR spectrometer for reflection–absorption infrared spectroscopy (RAIRS), and the QCM for thin-film mass determination. The grain mimic is an uncharacterized gold film surface, suspended at the end of a cryogenic cold finger, capable of reaching 7 K. The sample is radiatively heated from the reverse side by a halogen bulb. The sample temperature is measured using two E-type (Ni–Cr alloy versus Cu–Ni alloy) and one KP-type (Au including 0.7 per cent Fe versus Chromel) thermocouples, positioned on or near to the sample. The temperature can be controlled to better than 0.5 K, and measured accurately to within 0.25 K. The upper temperature range of the system is 350 K. The whole system is linked via data acquisition (DAQ) card, General Purpose Interface Bus (GPIB) and RS232 communications to a pair of PCs, which are used to coordinate and control data acquisition from various instruments on the experiment.

2.1 Deposition

H_2O was obtained *in situ* from a liquid H_2O sample that had been deionized, filtered for organic and inorganic solutes, and subjected to three freeze–thaw cycles under a vacuum of better than 1×10^{-7} torr. H_2O ice films were deposited at a rate of *c.* 10^{10} molecules $\rm s^{-1}$ on the gold film substrate held at a temperature of 10 K, from a quasi-effusive molecular beam of H_2O, directed at 5° to the surface normal. At such low temperatures and low deposition rates ballistic deposition results in the formation of high-density amorphous ice. Exposure of the substrate to gaseous H_2O was varied between 1 and 100 Langmuir (L) (1 Langmuir is equivalent to 1×10^{-6} torr s), and film mass was estimated using the QCM. An exposure of 20 L corresponded to a film mass of $\approx 3.8 \times 10^{-7}$ g, which equates to a surface number density of H_2O of 2.44×10^{16} molecules $\rm cm^{-2}$, or a film thickness of ≈0.03 μm, when proper account of the QCM sensor area is made.

2.2 Temperature-programmed desorption

The sublimation characteristics of the H_2O films were measured by temperature-programmed desorption (TPD). In this method a linear temperature ramp is applied to the sample and the rate of desorption is measured by monitoring the amount of adsorbate that desorbs into the gas phase as a function of temperature. Desorption is an activated process which takes place at a rate given by

$$R = -\,{\rm d}N_{\rm S}/{\rm d}t = k_{\rm d} N_{\rm S}^{m}, \tag{1}$$

where $N_{\rm S}$ is the number of adsorbed molecules on the surface in molecules $\rm cm^{-2}$, m is the order of the reaction and $k_{\rm d}$ is the rate constant, given by

$$k_{\rm d} = A \exp(-E_{\rm des}/k_{\rm B}T), \tag{2}$$

where A is the pre-exponential factor, $E_{\rm des}$ is the binding energy of a molecule on the ice surface in joules, $k_{\rm B}$ is the Boltzmann constant and T is the ice temperature in kelvin. For convenience, in this paper the surface binding energies are expressed as $E_{\rm des}/k_{\rm B}$, i.e. in kelvin, and the units of A are determined from $k_{\rm d}$: i.e. for $m = 1$, A is expressed in $\rm s^{-1}$; and where $m = 0$, A is expressed in molecules $\rm cm^{-2}\,s^{-1}$. Equation (1) can be rewritten, to reflect the TPD signal that is actually measured during the experiment, i.e.

$$-\,{\rm d}N_{\rm S}/{\rm d}T = k_{\rm d}(N^{m}/\beta), \tag{3}$$

where β is the heating rate, ${\rm d}T/{\rm d}t$. The recorded TPD signal peaks

at some temperature maximum, T_d, which corresponds to the point at which the desorption rate from the surface is at a maximum, i.e. $d^2N_S/dt^2 = 0$. The TPD spectra are collected at increasing initial surface coverages, using the same linear heating ramp in each case. To a first approximation, the surface binding energy, E_{des}, can then be calculated directly by substituting for k_d in equation (3) (using equation 2), differentiating and equating to zero:

$$E_{des}/k_B T_d^2 = (A/\beta) m N_S^{m-1} \exp(-E_{des}/k_B T_d), \quad (4)$$

provided that the pre-exponential factor, A, is known. In a first-order desorption process, where $m = 1$, A is assumed to be around $10^{12}-10^{13}\,s^{-1}$, approximately the vibrational frequency of the weak bond between the adsorbate molecule and the surface. It is also possible to evaluate the order of the reaction from the TPD peak shape and peak maximum provided that the activation energy for desorption and the pre-exponential factor remain constant as a function of surface coverage. In practice, however, desorption may not occur in a single step, the surface binding energy can vary across binding sites on the surface or with surface coverage, and the pre-exponential factor, A, may differ by several orders of magnitude. A more rigorous result can be obtained by modelling the desorption system and using numerical fitting methods with a number of TPD spectra to evaluate the values of A and E_{des} [see Woodruff & Delchar (1986) and Attard & Barnes (1998) for a more complete discussion].

In these experiments the ice layers were warmed at a rate of $0.02\,K\,s^{-1}$ and the QMS, tuned to mass 18 (H_2O^+), was used to monitor the gas-phase composition during desorption from the substrate. The QMS was operated in a line-of-sight configuration so that only molecules originating from the sample surface produced a signal at the detector (Fisher & Jones 1999). Sample coverages of 1, 2, 5, 10, 20 and 50 L (submonolayer to multilayer) were used. In all cases, no desorption was observed before 120 K and desorption was complete by 170 K.

3 RESULTS

Fig. 1 shows a sequence of TPD spectra for H_2O films deposited at 10 K, with increasing surface coverage. The spectra show the change in intensity of the mass 18 (H_2O^+) signal at the QMS as the sample is slowly heated. An intense, asymmetric peak is observed at ≈140 K, associated with the desorption of the bulk ice film from the Au substrate. There is little or no change in the shape of the leading edge peak with increasing exposure. Furthermore, the peak temperature, T_d, increases monotonically with exposure. These observations are typical of TPD spectra in which the desorption process follows zeroth-order kinetics, as illustrated by Fig. 2. The figure shows results from a series of (a) zeroth- and (b) first-order TPD simulations (based on equation 3), at coverages of 2, 5, 10, 20, 50 and 100 monolayers of H_2O, and under conditions similar to

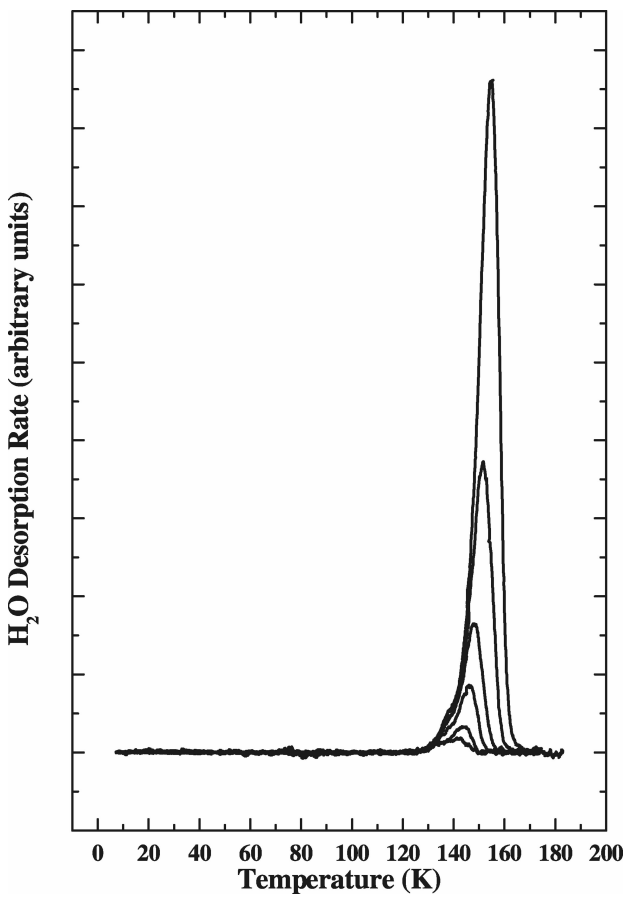

Figure 1. TPD spectra for H_2O ice films deposited at 10 K on an Au substrate. Spectra are shown for surface exposures of 1, 2, 5, 10, 20 and 50 L (in order of increasing intensity). See text for details.

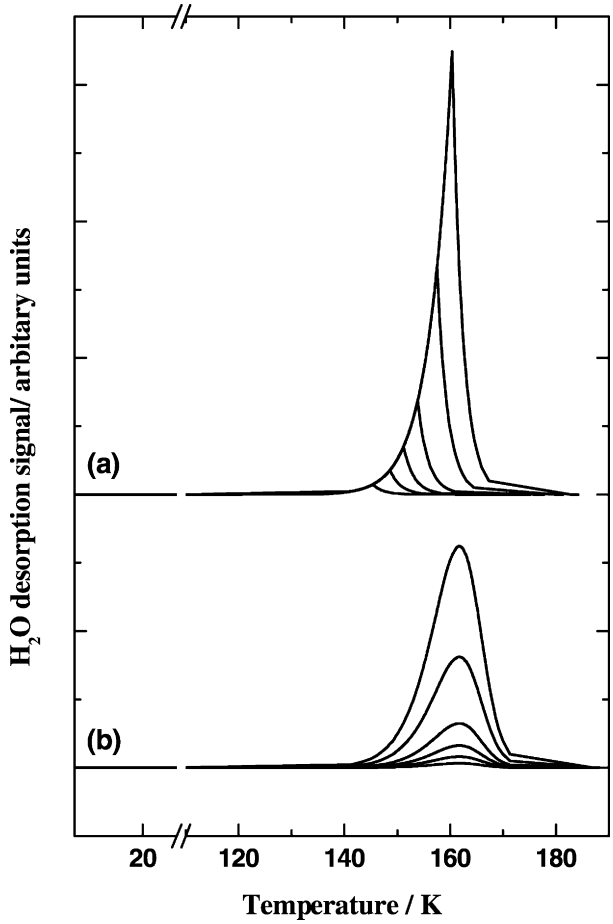

Figure 2. TPD spectra from a series of (a) zeroth-order ($A = 10^{30}$ molecules $cm^{-2}\,s^{-1}$) and (b) first-order ($A = 10^{13}\,s^{-1}$) simulations (based on equation 3), at coverages of 2, 5, 10, 20, 50 and 100 monolayers of H_2O (in order of increasing intensity). In each case, the desorption energy, E_{des}, was fixed at 5773 K, and the heating ramp, β, was $0.01\,K\,s^{-1}$.

those in this experiment. In the zeroth-order case (Fig. 2a), the TPD curves are asymmetric, with coincident rising edges, and the peak temperature, T_d, increases with exposure. This is typical of multilayer desorption, where the intensity of the TPD spectrum increases as more and more material is condensed on to the surface. The shift in T_d (the peak position) occurs because the desorption rate increases exponentially with temperature, so the rate can increase indefinitely until all the layers have been stripped away, and the TPD signal falls rapidly to zero. The bonding between the layers resembles that in a condensed solid of the adsorbate, so the desorption energy, E_{des}, and pre-exponential factor, A, are the same for every layer. In contrast, the first-order desorption curves are symmetric about a single T_d value, independent of coverage (see Fig. 2b). This closely resembles monolayer desorption kinetics, when the nature of the bonding between the adsorbate and the underlying substrate is clearly important. In a multilayer system (e.g. icy mantles on dust grains, or the ice system studied here) the monolayer is generally more tightly bound to the underlying substrate than to the subsequent adsorbate layers. Consequently, the monolayer desorption peak appears at higher temperatures in the TPD spectrum than the multilayer desorption, reflecting a different E_{des} value. Its line shape profile will also differ, reflecting both a different A value and the different reaction kinetics. A more complete discussion of this complex relationship between TPD line shape profiles, binding energies and desorption kinetics can be found in Woodruff & Delchar (1986) or Attard & Barnes (1998). However, from a comparison between the experimental TPD spectra presented in Fig. 1 and the simulations in Fig. 2, it is reasonable to conclude that the results of this experiment are indicative of zeroth-order kinetics. Furthermore, only a single peak is observed in the TPD spectra: even at low coverage it is not possible to deconvolve a monolayer desorption peak from the multilayer peak. Therefore no evidence exists to suggest that the desorption process is coverage-dependent, nor that it is possible to distinguish between the multilayer and monolayer desorption processes. These observations are entirely consistent with previous reports on the TPD of ice from other hydrophobic, metal substrates (Kay et al. 1989; Dohnálek et al. 1999, 2000).

In some cases, and particularly at higher exposure, a slight shoulder is observed on the leading edge of the 140-K TPD peak. Under these experimental conditions, the phase transition between amorphous and crystalline ice is known to occur between 120 and 140 K (Sack & Baragiola 1993). It might be expected, therefore, that all the desorbing ice should be in the crystalline phase by the time that desorption occurs. However, given the relatively long time-scale for this phase change (Dohnálek et al. 2000), it is likely that some desorption will occur from the residual amorphous phase that has yet to undergo the phase change. The TPD peak of the amorphous ice will occur at a lower temperature than the main desorption peak, since the vapour pressure of the amorphous ice is around three times greater than that of crystalline ice (Kouchi 1987). This behaviour is clearly illustrated in Fig. 3. Traces (a) and (b) show the TPD spectra from H_2O films of equivalent surface exposure, deposited at two temperatures, 10 and 100 K, producing high-density amorphous ice and low-density amorphous ice, respectively. The films were cooled to 10 K and then treated as described in Section 2. Their TPD spectra are essentially equivalent, showing the amorphous ice desorption shoulder on the leading edge, which gradually flattens out as the crystallization phase change dominates, and finally the major TPD peak, corresponding to desorption of the crystalline phase. Two further films, with double the surface coverage of the amorphous films,

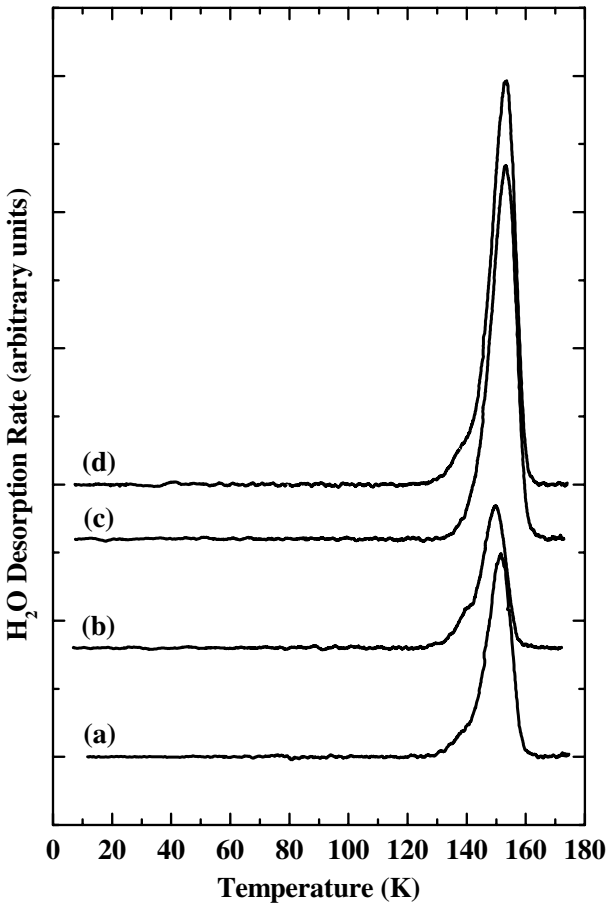

Figure 3. TPD spectra for H_2O ice films prepared (a) by 20-L exposure at 10 K, (b) by 20-L exposure at 100 K, (c) by 80-L exposure at 130 K, and (d) by 20-L exposure at 100 K followed by 20-L exposure at 10 K. Each film was then cooled to 10 K prior to desorption. Spectra are offset for clarity.

were also investigated. Trace (c) shows results for an H_2O film that was grown at 130 K, then cooled to 10 K and warmed. The TPD spectrum from this ice film is narrower, with the onset of desorption occurring slightly later than in the other spectra, and no evidence of the amorphous shoulder can be seen. These features are attributed to the purely crystalline nature of this ice film. Finally trace (d) in this spectrum was produced by depositing equal amounts of H_2O at 100 and then 10 K. The total surface coverage in (d) is therefore equivalent to (c). The TPD trace for this sample shows evidence of the amorphous phase desorption, but the phase change appears to be much faster than in (a) or (b), and the spectrum is dominated by desorption from the crystalline phase. Similar results have been found in previous studies of ice desorption from various substrates, where the rate of crystallization has also been determined (Smith et al. 1996; Speedy et al. 1996).

A kinetic model was used to evaluate the surface binding energy, E_{des}, and the pre-exponential factor, A, for the crystalline H_2O ice system. To model the kinetics of the bulk ice desorption, a simple reaction scheme was constructed to describe the desorption process:

$$H_2O\,(s) \xrightarrow{k_d} H_2O\,(g), \tag{5}$$

$$H_2O\,(g) \xrightarrow{k_p} \text{pump}, \tag{6}$$

where the concentration of H_2O (s) is equivalent to N_S, the number of adsorbed molecules on the surface, and k_p is the pumping coefficient of H_2O in this system. A zeroth-order rate equation,

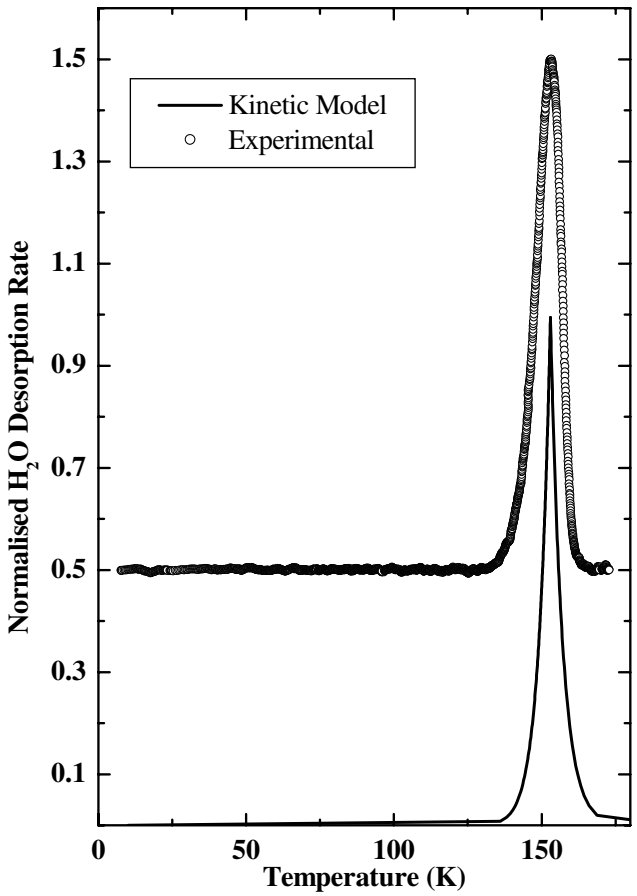

Figure 4. A comparison between experimental and modelled TPD spectra. See text for discussion.

based on equation (1), was used to describe the desorption of molecules into the gas phase:

$$\mathrm{d}[\mathrm{H_2O\,(g)}]/\mathrm{d}t = k_\mathrm{d}. \quad (7)$$

The rate coefficient, k_d, is equivalent to that described in equation (2). A similar first-order rate equation was used to describe equation (6):

$$\mathrm{d}[\mathrm{H_2O\,(g)}]/\mathrm{d}t = -k_\mathrm{p}[\mathrm{H_2O\,(g)}]. \quad (8)$$

The TPD spectrum then represents the temporal evolution of these coupled differential equations as the system temperature is raised in a linear manner. Using an initial H_2O ice surface density of 2.44×10^{16} molecules $\mathrm{cm^{-2}}$ (corresponding to a 20-L exposure), an initial temperature of 10 K, and a linear temperature ramp of $0.02\,\mathrm{K\,s^{-1}}$, model TPD spectra were calculated using a simple stochastic integration package[1] (Houle & Hinsberg 1995) and compared with the empirical data. The unknown parameters in the model, the surface binding energy, E_des, and the pre-exponential for desorption, A, were then varied to obtain the best reproduction of the empirical data. This was achieved for an A value of $10^{30\pm2}$ molecules $\mathrm{cm^{-2}\,s^{-1}}$ and an E_des value of 5773 ± 60 K. Fig. 4 shows the comparison of the model results with the empirical data.

It is much more complicated to evaluate the A and E_des values of the amorphous phase as the desorption and crystallization processes are occurring simultaneously. To evaluate the gas-phase H_2O concentration as measured in the experiment, it is necessary to couple equations describing the amorphous ice desorption rate and the crystallization rate to equations (6) and (7). This work is currently ongoing, and will be the subject of a later paper. From the shapes and behaviour of the TPD curves in Figs 1 and 3, however, it is clear that the desorption mechanism for the amorphous ice is identical to that of the crystalline ice. Previous studies have drawn the same conclusion (Dohnálek et al. 1999, 2000). Initial results from our model suggest that the A factor for amorphous ice is of the same order of magnitude as, and E_des is a few hundred kelvin lower than, that of crystalline ice.

[1]Chemical Kinetics Simulator (CKS), Version 1.0, IBM Almaden Research Center, 650 Harry Road, Mailstop ZWX1D1, San Jose, CA, USA. Further information may be obtained from the CKS website at http://www.almaden.ibm.com/st/msim/ckspage.html

4 ASTROPHYSICAL IMPLICATIONS

The results obtained here compare favourably to previous TPD measurements of H_2O desorption under UHV conditions, from a range of surfaces (Kay et al. 1989; Haynes, Tro & George 1992; Smith, Huang & Kay 1997; Chakarov & Kasemo 1998; Dohnálek et al. 1999, 2000). Where values for E_des and A are provided, the data are summarized in Table 1, where a comparison is also made with the spectroscopic results of Sandford & Allamandola (1988). With the exception of the latter results, the table clearly shows that, for both ordered and disordered hydrophobic surfaces, the desorption energy and rate constant are independent of the substrate. In each case, the desorption kinetics resemble zeroth-order rather than first-order reaction kinetics.

None of the studies mentioned in Table 1 has identified any differences between the desorption of H_2O from H_2O layers and the desorption of H_2O from the underlying substrate. This indicates that H_2O is only weakly bound to hydrophobic substrates, and that the adsorbate–substrate binding energy is comparable to the adsorbate–adsorbate hydrogen bonding. In astrophysical terms, this indicates that the same desorption mechanism and desorption energy can be used to model H_2O desorption from any hydrophobic surface (e.g. silicon, graphite). Similar desorption studies on hydrophilic surfaces (such as metal oxides, quartz and silicates) indicate that H_2O bonds chemically to such surfaces. In such cases, the H_2O–substrate system exhibits alternative desorption kinetics, with even higher activation barriers (e.g. Stirniman et al. 1996; Trakhtenberg et al. 1997; Hudson et al. 2001). However, these systems do exhibit identical H_2O–H_2O desorption processes in the regime where the ice surface is substrate-independent (i.e. the ice layer is thick enough that it is no longer influenced by the underlying substrate). Consequently, in ISM regions where relatively thick ice layers are formed, or the grain surface is hydrophobic, the underlying structure of the cosmic grain is not significant. Elsewhere, the grain material may influence the H_2O desorption mechanism. It will not be possible to say conclusively which H_2O desorption kinetics will dominate until the nature of interstellar grains has been clearly established.

As Table 1 shows, the results obtained in this study differ significantly from those obtained by Sandford & Allamandola (1988). First, E_des differs by ≈ 800 K for both the crystalline and amorphous ice phases; secondly, the desorption kinetics in this study are clearly zeroth-order and not first-order. These two parameters are both significant when modelling interstellar environments, particularly when calculating the residence time of H_2O on interstellar grains, or establishing the ratio of solid to gas-phase material.

Why do the two methods give such different results? The

Table 1. A comparison of surface binding energy, E_{des}, and pre-exponential factor, A, measurements for (a) crystalline ice and (b) amorphous ice.

Substrate	Au[a]	Ru (001)/ Au (111)[b]	Sapphire[c]	CsI[d]
(a) Crystalline ice				
E_{des} (K)	5773 ± 60	5803 ± 96	5989	5070 ± 50
$A \times 10^{30}$ (molecules $cm^{-2} s^{-1}$)	1	4.58	2.8	$*2 \times 10^{12} s^{-1}$
m	0	0	0	1
(b) Amorphous ice				
E_{des} (K)	≈ 5600	5640 ± 96		4815 ± 15
$A \times 10^{30}$ (molecules $cm^{-2} s^{-1}$)	≈ 1	3.75		$*2 \times 10^{12} s^{-1}$
m	0	0		1

* Units of s^{-1}, not molecules $cm^{-2} s^{-1}$, as reaction was assumed to be first- and not zeroth-order.
References: [a] this work; [b]Speedy et al. (1996); [c]Haynes et al. (1992); [d]Sandford & Allamandola (1988).

discrepancies must be related to the different assumptions that are made in interpreting the data under each set of experimental conditions. The most significant difference between the two experiments is that the spectroscopic data are taken under isothermal conditions at base pressures of $\approx 2 \times 10^{-8}$ torr, whereas the TPD spectra are recorded in dynamic conditions at base pressures of 6×10^{-11} torr. In the spectroscopic measurements, it was assumed that a first-order rate law applied, and the value of E_{des} was determined indirectly, by monitoring the relative change in integrated intensity of a surface infrared spectroscopic feature during isothermal desorption. Contrary to the assumptions made in Sandford & Allamandola's method, close to the desorption temperature, the sticking probability of H_2O molecules on the surface is no longer unity, and over the time period of the experiment it is possible for re-adsorption to occur, from both vacuum contaminants and desorbing gas. The evaluation of isothermal measurements is also complicated by non-equilibrium effects, including both crystallization and re-adsorption. In the TPD experiments it is possible to obtain information on the order of the reaction and E_{des} directly, from the shape and position of the TPD curve. In UHV systems designed for TPD experiments, the pumping speed is so high that surface re-adsorption is not relevant. Unlike the spectroscopic data, the TPD spectra clearly show that crystallization and desorption are occurring concurrently in the system. It is possible, however, to distinguish the amorphous, crystalline and 'phase change' regions of the TPD spectra from each other. With careful film preparation it is even possible to force the TPD spectrum to exhibit only crystalline behaviour, as was seen in Fig. 3. Furthermore, Kay and co-workers have made a number of studies using TPD methods to determine the rates of crystallization and desorption when they are occurring at the same time, and have found no significant difference between the desorption rates that they measure isothermally or dynamically (Smith et al. 1996; Speedy et al. 1996; Dohnálek et al. 1999, 2000). Finally, the experimental conditions under which the TPD spectra were obtained most closely resemble those in the ISM. We therefore believe that these data represent the parameters for H_2O that should be employed in astronomical models.

Table 2 shows the effect that these new parameters have on the 'residence times' of H_2O molecules on H_2O ices and hydrophobic surfaces. It is not possible to define a residence time for a zeroth-order process that is directly comparable (with the same units) with a first-order process. Consequently, the results are presented here in terms of the half-life of the H_2O surface population, rather than the 'residence time, $1/k_d$' that is commonly used in the astronomical literature. The respective half-life values are defined in the table. It is important to note that the half-life of a zeroth-order process also depends on the surface concentration of H_2O molecules. In these calculations this value was fixed at 1.15×10^{17} molecules cm^{-2}, equivalent to around 100 monolayers of H_2O ice, i.e. the number of H_2O layers expected to accrete on a interstellar grain during the lifetime of a dense cloud (Hasegawa & Herbst 1993). The half-lives calculated using the zeroth-order A and E_{des} values obtained in this work are given in bold in columns 1 (crystalline ice) and 3 (amorphous ice). The results are also compared with half-life calculations using the data from Sandford & Allamandola (1993). The half-lives calculated using Sandford & Allamandola's first-order A and E_{des} values are given in columns 6 (crystalline ice) and 8 (amorphous ice). From Table 2 it is immediately clear that H_2O can remain on the grain surface at significantly higher temperatures than has previously been assumed, typically around 110–120 K rather than 90–100 K.

5 CONCLUSIONS

The surface binding energy and desorption kinetics of amorphous and crystalline H_2O ice have been studied under conditions similar to those found in denser regions of interstellar clouds. These data have been used to calculate the residence times of H_2O on H_2O and hydrophobic surfaces as a function of temperature. The results imply that, in the dense interstellar medium, thermal desorption of H_2O ice will occur at significantly higher temperatures, and different rates, than previously had been assumed. These data are of fundamental importance in the chemical modelling of many astrophysical environments. The effects may be particularly pronounced in so-called hot cores, which are very dense clumps of gas, remnants of a collapsing cloud that formed a massive star. Irradiation of the clumps heats the cores to temperatures in the range 100–300 K, when the ices evaporate, populating the gas with water and other trace molecules (cf. Millar 1993). The temperature of the evaporation may be crucial to relating the observed chemistry of hot cores to the implied rate of warming of the central star (Viti & Williams 1999). The results provide the astronomical

Table 2. The half-life, $t_{1/2}$, of H_2O molecules on H_2O ice surfaces as a function of temperature under zeroth- and first-order kinetics. In each case, the half-life is defined in the table, and represents the time that it takes for the surface population of H_2O molecules on an interstellar grain to decrease to one-half of its initial value. Bold text indicates data calculated using results from this work.

Grain T (K)	Half-life, $t_{1/2}$ (yr)							
	Zeroth-order desorption kinetics, i.e. $t_{1/2} = N_{S,0}/2k_d$ where $N_{S,0} = 1.15 \times 10^{17}$ molecules cm^{-2} s^{-1}				First-order desorption kinetics, i.e. $t_{1/2} = \ln 2/k_d$			
	H_2O on crystalline ice		H_2O on amorphous ice		H_2O on crystalline ice		H_2O on amorphous ice	
	(a)	(b)	(a)	(b)	(c)	(d)	(c)	(d)
10	$\mathbf{8.8\times10^{231}}$	1.3×10^{200}	$\mathbf{6\times10^{224}}$	8.9×10^{188}	4.6×10^{232}	6.8×10^{200}	3.8×10^{225}	5.7×10^{189}
20	$\mathbf{8.6\times10^{105}}$	1×10^{90}	$\mathbf{2\times10^{102}}$	2.5×10^{84}	4.5×10^{106}	5.5×10^{90}	1.3×10^{103}	1.6×10^{85}
30	$\mathbf{8.5\times10^{63}}$	2.1×10^{53}	$\mathbf{3\times10^{61}}$	3.5×10^{49}	4.5×10^{64}	1.1×10^{54}	2×10^{62}	2.2×10^{50}
40	$\mathbf{8.4\times10^{42}}$	9.3×10^{34}	$\mathbf{1.2\times10^{41}}$	1.3×10^{32}	4.4×10^{43}	4.9×10^{35}	7.6×10^{41}	8.3×10^{32}
50	$\mathbf{2.1\times10^{30}}$	9.1×10^{23}	$\mathbf{6.7\times10^{28}}$	4.5×10^{21}	1.1×10^{31}	4.8×10^{24}	4.3×10^{29}	2.9×10^{22}
60	$\mathbf{8.4\times10^{21}}$	4.2×10^{16}	$\mathbf{4.6\times10^{20}}$	4.9×10^{14}	4.4×10^{22}	2.2×10^{17}	2.9×10^{21}	3.1×10^{15}
70	$\mathbf{8.4\times10^{15}}$	2.4×10^{11}	$\mathbf{6.7\times10^{14}}$	5.1×10^{9}	4.4×10^{16}	1.3×10^{12}	4.3×10^{15}	3.3×10^{10}
80	$\mathbf{2.7\times10^{11}}$	2.8×10^{7}	$\mathbf{2.8\times10^{10}}$	9.4×10^{5}	1.4×10^{12}	1.5×10^{8}	1.8×10^{11}	6.1×10^{6}
90	$\mathbf{8.4\times10^{7}}$	2.4×10^{4}	$\mathbf{1.1\times10^{7}}$	1.2×10^{3}	4.4×10^{8}	1.3×10^{5}	7.2×10^{7}	7.5×10^{3}
100	$\mathbf{1.3\times10^{5}}$	8.7×10^{1}	$\mathbf{2.1\times10^{4}}$	5.6×10^{0}	7×10^{5}	4.6×10^{2}	1.4×10^{5}	3.6×10^{1}
110	$\mathbf{6.8\times10^{2}}$	8.7×10^{-1}	$\mathbf{1.3\times10^{2}}$	7×10^{-2}	3.6×10^{3}	4.6×10^{0}	8.1×10^{2}	4.5×10^{-1}
120	$\mathbf{8.4\times10^{0}}$	1.8×10^{-3}	$\mathbf{1.8\times10^{0}}$	1.9×10^{-2}	4.1×10^{1}	9.8×10^{-2}	1.1×10^{1}	1.2×10^{-2}
130	$\mathbf{2\times10^{-1}}$	7.2×10^{-4}	$\mathbf{4.7\times10^{-2}}$	8.3×10^{-5}	1.1×10^{0}	3.8×10^{-3}	3.1×10^{-1}	5.3×10^{-4}
140	$\mathbf{8.4\times10^{-3}}$	5.9×10^{-6}	$\mathbf{2.1\times10^{-3}}$	4.5×10^{-5}	4.2×10^{-2}	2.3×10^{-4}	1.4×10^{-2}	3.8×10^{-5}
150	$\mathbf{5.3\times10^{-4}}$	4×10^{-6}	$\mathbf{1.5\times10^{-4}}$	6×10^{-7}	2.8×10^{-3}	2.1×10^{-5}	9.4×10^{-4}	3.8×10^{-6}

(a) E_{des} and A taken from this work.
(b) E_{des} taken from Sandford & Allamandola (1988); A taken from this work.
(c) E_{des} taken from this work; A taken from Sandford & Allamandola (1988).
(d) E_{des} and A taken from Sandford & Allamandola (1988).

community with reliable thermodynamic data pertaining to the desorption of H_2O under interstellar conditions.

ACKNOWLEDGMENTS

The authors thank PPARC for their financial support, without which these experiments would not have been possible.

REFERENCES

Attard G., Barnes C., 1998, Surfaces. Oxford Univ. Press, Oxford
Chakarov D., Kasemo B., 1998, Phys. Rev. Lett., 81, 5181
Dohnálek Z., Ciolli R. L., Kimmel G. A., Stevenson K. P., Smith R. S., Kay B. D., 1999, J. Chem. Phys., 110, 5489
Dohnálek Z., Ciolli R. L., Kimmel G. A., Stevenson K. P., Smith R. S., Kay B. D., 2000, J. Chem. Phys., 112, 5932
Ehrenfreund P., Schutte W. A., 2000, in Minh Y. C., van Dishoeck E. F., eds, Proc. IAU Symp. 197, Astrochemistry: From Molecular Clouds to Planetary Systems. Astron. Soc. Pac., Provo, p. 135
Fisher C., Jones R. G., 1999, Surf. Sci., 424, 127
Fraser H. J., Collings M. P., McCoustra M. R. S., 2001, Rev. Sci. Instrum., in press
Hasegawa T. I., Herbst E., 1993, MNRAS, 261, 83
Haynes D. R., Tro N. J., George S. M., 1992, J. Phys. Chem., 96, 8502
Houle F. A., Hinsberg W. D., 1995, Surf. Sci., 338, 329
Hudson P. K., Foster K. L., Tolbert M. A., George S. M., Carlo S. R., Grassian V. H., 2001, J. Phys. Chem. A, 105, 694
Jenniskens P., Blake D. F., 1994, Sci, 265, 753
Jenniskens P., Blake D. F., 1996, ApJ, 473, 1104
Jenniskens. P., Blake D. F., Wilson M. A., Pohorille A., 1995, ApJ, 455, 389
Jenniskens. P., Banham S. F., Blake D. F., McCoustra M. R. S., 1997, J. Chem. Phys., 107, 1232
Kay B. D., Lykke K. R., Creighton J. R., Ward S. J., 1989, J. Chem. Phys., 91, 5120
Kouchi A., 1987, Nat, 330, 550
Millar T. J., 1993, in Millar T. J., Williams D. A., eds, Dust and Chemistry in Astronomy. IoP Publishing, Bristol, p. 249
Rawlings J. M. C., 2000, in Minh Y. C., van Dishoeck E. F., eds, Proc. IAU Symp. 197, Astrochemistry: From Molecular Clouds to Planetary Systems. Astron. Soc. Pac., Provo, p. 15
Sack N. J., Baragiola R. A., 1993, Phys. Rev. Lett., 48, 9973
Sandford S. A., Allamandola L. J., 1988, Icarus, 76, 201
Sandford S. A., Allamandola L. J., 1993, ApJ, 417, 815
Smith R. S., Huang C., Wong E. K. L., Kay B. D., 1996, Surf. Sci., 367, L13
Smith R. S., Huang C., Kay B. D., 1997, J. Phys. Chem. B, 101, 6123
Speedy R. J., Debenedetti P. G., Smith R. S., Huang C., Kay B. D., 1996, J. Chem. Phys., 105, 240
Stirniman M. J., Huang C., Smith R. S., Joyce S. A., Kay B. D., 1996, J. Chem. Phys., 105, 1295
Trakhtenberg S., Naaman R., Cohen S. R., Benjamin I., 1997, J. Phys. Chem. B, 101, 5172
van Dishoeck E. F., van der Tak F. F. S., 2000, in Minh Y. C., van Dishoeck E. F., eds, Proc. IAU Symp. 197, Astrochemistry: From Molecular Clouds to Planetary Systems. Astron. Soc. Pac., Provo, p. 97
Viti S., Williams D. A., 1999, MNRAS, 305, 755
Whittet D. C. B., 1993, in Millar T. J., Williams D. A., eds, Dust and Chemistry in Astronomy. IoP Publishing, Bristol, p. 9
Williams D. A., 1998, Faraday Discuss., 109, 1
Woodruff D. P., Delchar T. A., Modern Techniques of Surface Science. Cambridge Univ. Press, Cambridge